International Research Journal of Engineering and Technology (IRJET) e-ISSN: 2395-0056
Volume: 07 Issue: 08 | Aug 2020 www.irjet.net p-ISSN: 2395-0072

A REVIEW ON NOSE CONE DESIGNS FOR DIFFERENT FLIGHT REGIMES

Aditya Rajan Iyer[1], Anjali Pant[2]

[1,2]*Students, Jain University International Institute of Aerospace Engineering and Management, Bangalore- 560078*

Abstract – In this paper we shall look into different nose cone designs primarily for high performance vehicles, what are the factors that a designer has to keep in mind in order to aerodynamically optimize them and what criteria has to be kept in mind so as to choose an appropriate geometry for the defined mission profile.

Key Words:

C_P - Centre of pressure

C_D - drag coefficient

γ - Ratio of specific heats

L - Length

V - Volume

M - Mach number

S_w - wetted area

C_{Dsf} - Skin friction coefficient

C_{D0} - zero lift drag

C_{WV} - Wave drag coefficient

C_{DB} - Base drag coefficient

P_b - Static pressure of base

P_∞ - Free stream static pressure

1. INTRODUCTION

Modern flight vehicles such rocket, missiles and airplanes due to their mission profiles experience performance degrading effects which need to be curbed. It is very important as designers that we figure out what could be the reasons for performance inhibition, and must find suitable methods or optimization techniques, so as to eliminate or minimize these effects. Also optimized aerodynamic variables lead to optimized trajectories, which play a vital role in payload delivery to the target.

In this survey we would be looking different nose cone geometries and study the various performance deterioration factors and their causes in different flow regimes, so that suitable nose cone geometries can be chosen in accordance to the mission profile.

The first problem that we would be addressing in this survey is to select the appropriate nose cone geometry which is best suited for specific flow and operating conditions. The selected nose cone geometry must have desirable drag, C_P **and heat transfer characteristics**. For this we would be using analytical & computational techniques to draw reasonable conclusions and results.

2. NOSE CONE GEOMETRIES

In designing a missile system there various configurations and designs that can be considered. Normally the shape and geometry of the nose cone is selected in the basis of combined considerations of aerodynamic, guidance and structure. In this section we would be briefly looking into various nose cone geometries used for vehicle design.

For an engineering problem statement we would be defining sections which are meant to travel through a compressible flow medium creating a solid of revolution shape which experiences minimal resistance through rapid motion in the fluid medium, as nose cone geometric shape greatly influences performance.

Conic, spherically blunted conic, bi-conic, tangent ogive, spherically blunted tangent ogive, secant ogive, elliptic, parabolic, power series and Haack series are the cone designs generally used for aerospace applications. The **Von-Karman** nose cone is a special case of the Haack series.

Fig-1 ¾ parabolic nose cone.

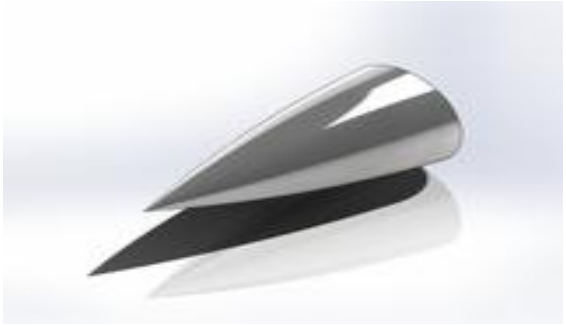

Fig-2 power series nose cone, n=3/4.

2.1. EFFECT OF NOSE CONE PROFILE ON AERODYNAMIC CHARECTERISTICS

For aircraft and rockets, below Mach 0.8, the nose pressure drag is essentially zero for all shapes. The major significant factor is friction drag, which is largely dependent upon the wetted area, the surface smoothness of that area, and the presence of any discontinuities in the shape. For subsonic rockets a short, blunt, smooth elliptical shape is usually best, but for transonic region and beyond, where the pressure drag increases dramatically, the effect of nose shape on drag becomes highly significant. The factors influencing the pressure drag are the **general shape** of the nose cone, **fineness ratio**, and its **bluffness ratio.**

The ratio of the length of a nose cone compared to its base diameter is known as the fitness ratio. Fineness ratio is often applied to the entire vehicle, considering the overall length and diameter. The length/diameter relation is also often called the **calibre** of a nose cone.

At supersonic speeds, the fineness ratio has a significant effect on nose cone **wave drag**, particularly at low ratios, but there is very little additional gain for ratios increasing beyond **5:1**. As the fineness ratio increases there is an increase in wetted area, and thus the **skin friction component of drag**, will also increase. Therefore, the minimum drag fineness ratio is ultimately going to be a trade-off between the decreasing **wave drag** and increasing **friction drag**.

Fig-3 Plot showing fitness ratio and wave drag

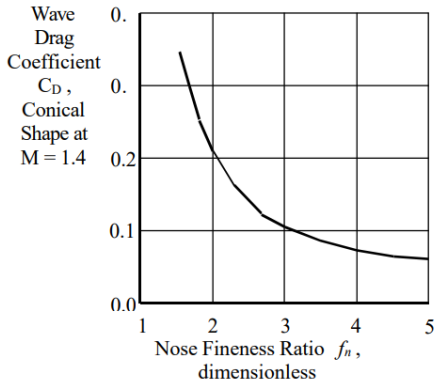

While most of the nosecone shapes ideally come to a sharp tip, they are often blunted to some degree as a practical matter for ease of manufacturing, resistance to handling and flight damage, and safety. **Bluffness Ratio** is often used to describe a **blunted tip**, and is equal to the **tip diameter** divided by the **base diameter**. Fortunately, there is little or no drag increase for slight blunting of a sharp nose shape. In fact, for constant overall lengths, there is a decrease in drag for bluffness ratios of up to 0.2, with an optimum at about 0.15. A flat truncation of a nose tip is known as a **Me plat diameter**, and the drag reduction effect of a **Me plat truncation** is shown in the diagram below.

Fig-4 Me plat truncation and Drag

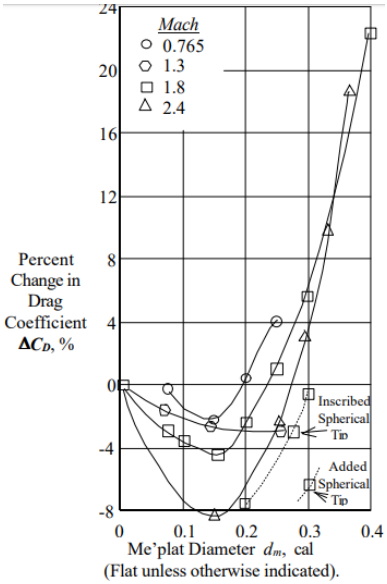

One of the main design factors that affect projectile configuration is the nose drag. The drag of the configurations is considered with respect to the Mach number. As fineness ratio and Mach number increases the overall drag decreases. Each drag component behaves differently depending on the Mach number and fineness ratio. The drag is compared

based on the 3 main drag components; skin friction drag, wave drag and base drag.

In general, there are three drag components, drag directly related to the cross-sectional of the projectile, **skin-friction drag** due to the contact between the surfaces of the projectile (roughness) with the surrounding air particles (viscosity), **wave drag** as a result of the shock wave and **base drag** as a result of bluntness and diameter of the base.

3. NOSE CONE FOR SUBSONIC FLOW

On looking into the subsonic flow regime, which is traversed by the vehicle during initial, the following plots and numerically generated contours help us understand the flow interaction with different nose cone profiles.

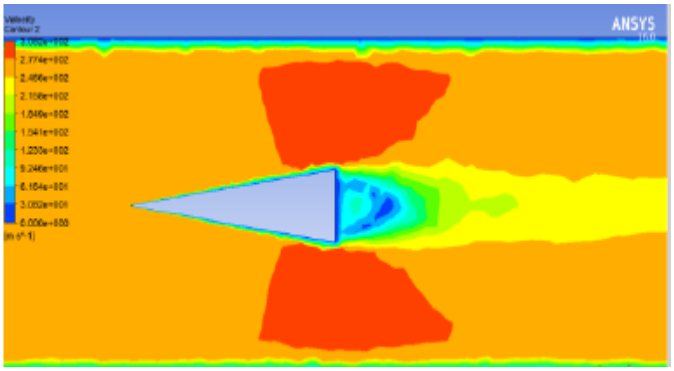

Fig-5 Conical at Mach 0.8

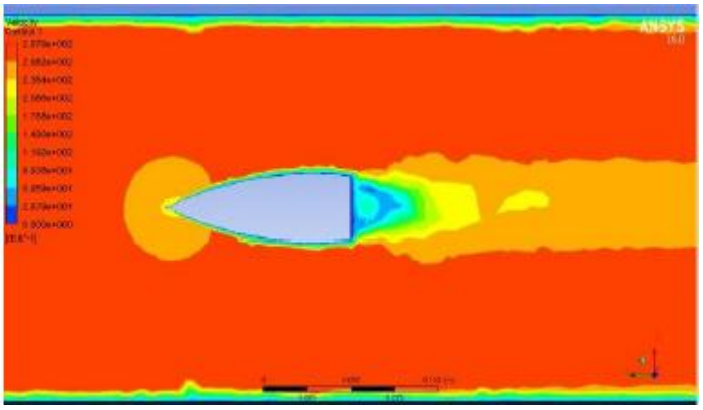

Fig-6 Velocity contour for parabolic section at Mach 0.8

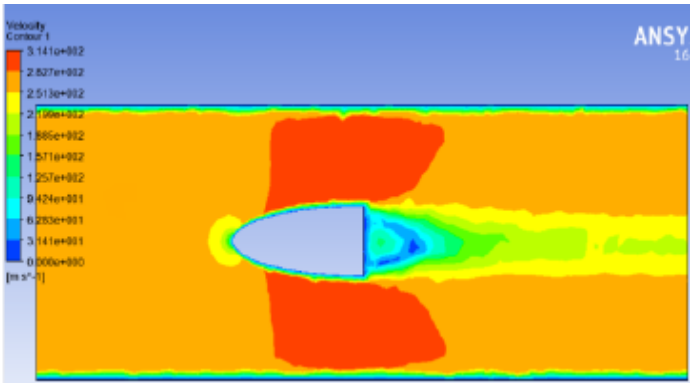

Fig-7 Velocity contour for ogive section at Mach 0.8

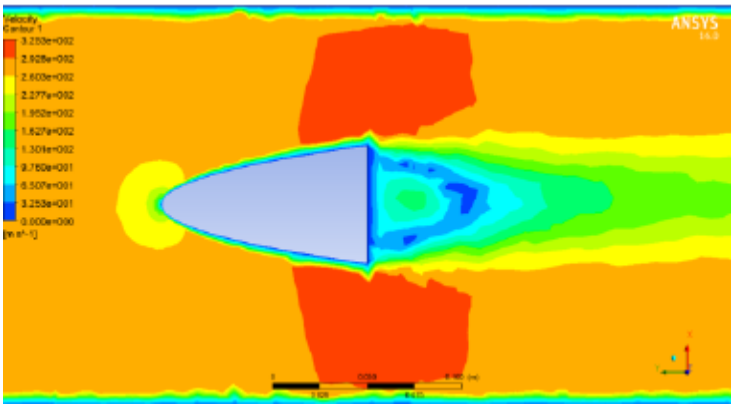

Fig-8 Velocity contour for elliptic section at Mach 0.8

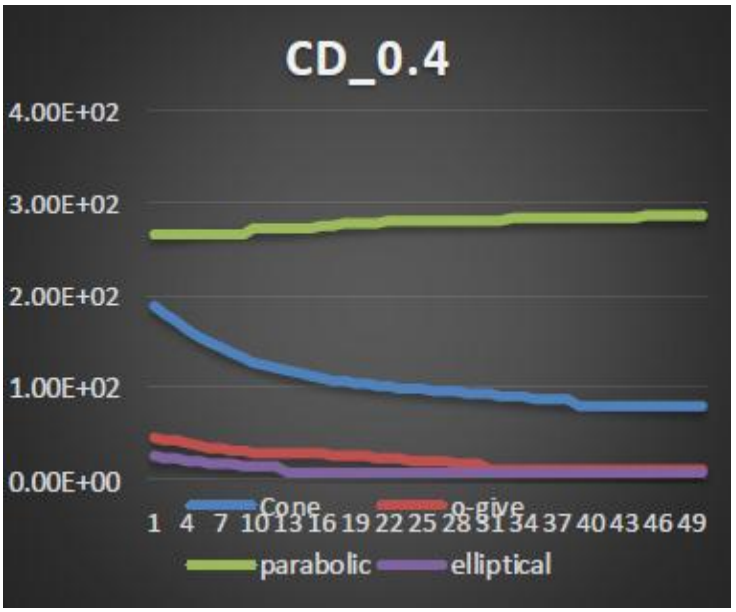

Fig-9 Plot showing C_D values at Mach 0.4

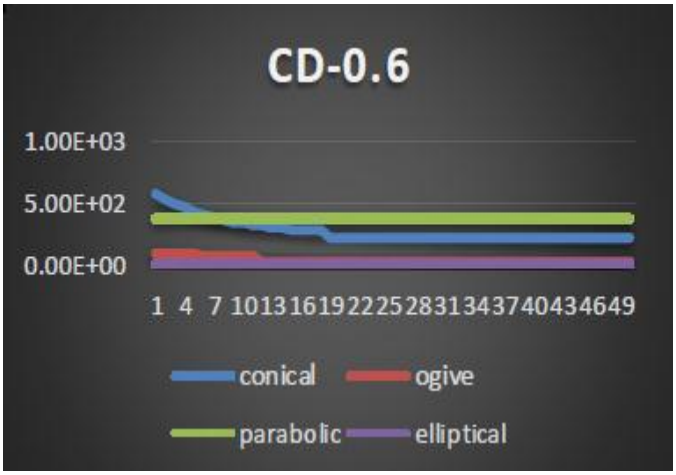

Fig-10 Plot showing C_D values at Mach 0.6

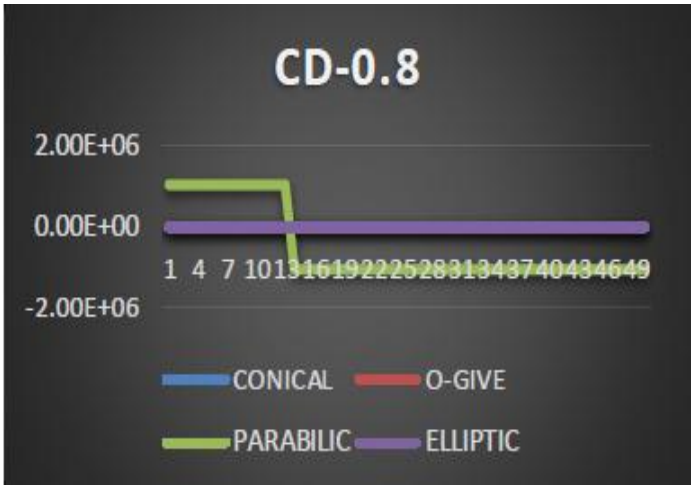

Fig-11 Plot showing C_D values at Mach 0.8

Going through the plots and the numerical simulations we can draw a reasonable conclusion that the **elliptic nose cone** profile gives a minimum drag coefficient although **parabolic** and **ogive** shapes can also be considered.

3.1 NOSE CONE FOR ABOVE MACH 0.8 TO TRANSONIC REGIME

Aerospace projects involve designing, building, and launching experimental sounding rockets or research rockets and missiles carrying payloads that perform scientific experiments in a sub-orbital trajectory that reach apogees up to 3 to 4 km. Throughout its trajectory within the atmosphere, they develop an adverse pressure gradient, that is, pressure increasing with increasing distance from the nose tip, will occur at some point along the fore body of the rocket. As the angle of attack is increased, the severity in the adverse pressure gradient on leeward side eventually induces boundary layer separation. A pair of vortices form, one on each side of the body forms at the start of leeward side boundary layer separation. As the vortex pair moves aft they will cause rolling moments on the tail fins of sounding rockets which can lead to roll lock-in or a catastrophic yaw. In roll lock-in the roll rate follows the pitch natural frequency. This prolonged resonance engenders excessive drag and structural loading with extremely adverse consequences to the mission.

For local supersonic flow occurs, returning to local subsonic conditions will be done by a normal shock wave. The onset of this phenomenon is when the local surface Mach number reaches unity. The free stream Mach number which corresponds to this is the critical Mach number. At higher speeds, the sudden jump to a lower Mach number across a normal shock will be accompanied by a jump in static pressure. Boundary layer separation can be postponed by employing a suitable shape and by increasing the static pressure at the fore body, the value of C_P also increases. Vortex mitigation and reduction in vortex strength can also be achieved through this, since the C_P local minimum is close to zero, the adverse gradient weakens.

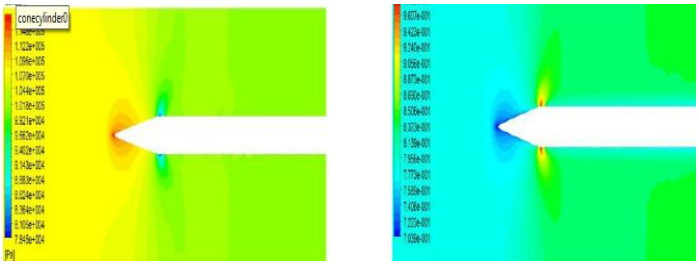

Fig-12 Pressure and Mach Contour for Conical nose cone.

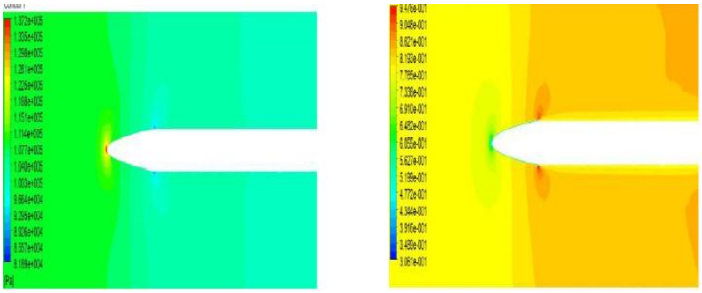

Fig-13 Pressure and Mach Contour for ogive nose cone.

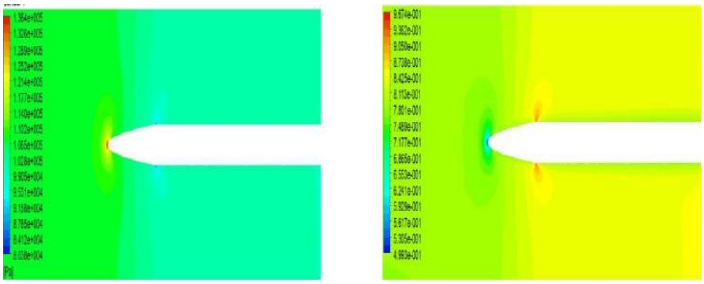

Fig-14 Pressure and Mach Contour for parabolic nose cone.

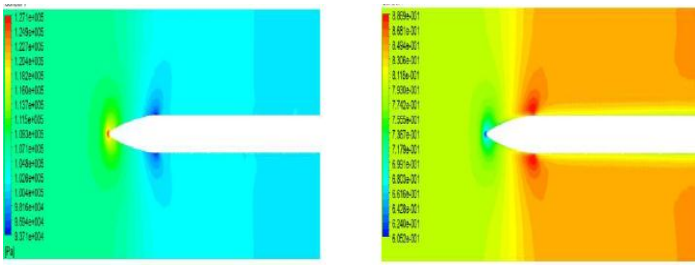

Fig-15 Pressure and Mach contours for Von Karman nose cone.

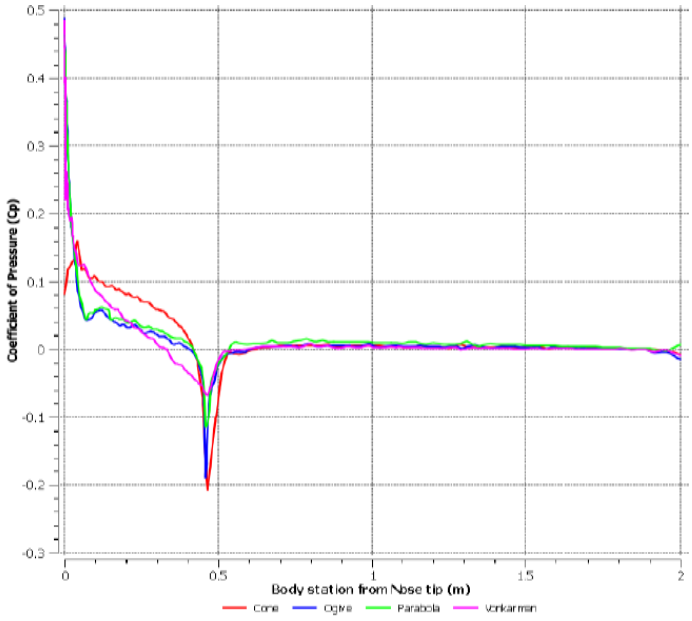

Fig-16 Showing C_p variation along the nose cone.

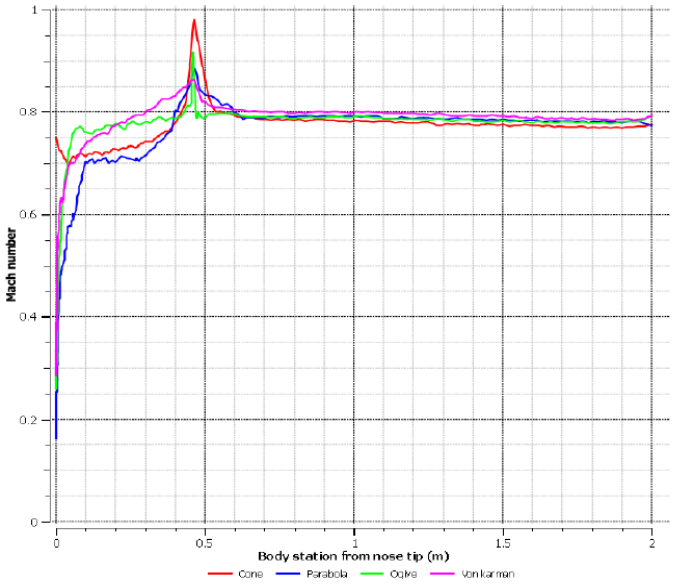

Fig-17 Showing Mach number variance along nose cone.

On evaluating the plots and the numerical contours it can be clearly seen that the **Von Karman** nose cone has least vortex strength. Because of its profile the flow is speeding slowly resulting in higher critical Mach number. Hence for flow operating conditions at Mach 0.8 or slightly above **Von Karman** would give us best results. Parabolic and ogive shapes can be considered for this regime.

4. NOSE CONE FOR SUPERSONIC FLOW REGIME

As previously discussed in the above sections drag primarily has 3 components the skin friction drag, wave drag and base drag all of which when taken in collective effect contribute to the total drag. There are analytical methods which are available through which we can calculate these three drag components:

$$C_{DO} = C_{Dw} + C_{Dsf} + C_{DB}$$

$$C_{Dsf} = \frac{4}{\pi} C_F S_w$$

$$C_{Dwv} = \frac{128 K_{vw} V^2}{\pi S L^4}$$

$$C_{DB} = \frac{2d^2{}_B}{\gamma M^2{}_\infty}\left(1 - \frac{P_b}{P_\infty}\right)$$

Zero lift drag coefficient basically describes the resistance of a particular body in the direction of the moving force or motion. The equation makes use of the **wetted area** and **viscosity** to determine the drag and is measured at **zero angle of attack. Skin-friction drag** is the result of viscous forces acting on the surface of the projectile, it also has high dependence on wetted area. **Wave drag** describes the drag due to the interaction of the body with the flow particles and is related to shockwave energy losses. **Base drag** is the drag formed from the base pressure as a result of the bluntness at the object and is highly dependent on the size of the base.

On referring to relevant literature a MATLAB code was written which generates plots for different components of drag and studies their variance with Mach number and fitness ratio. Fitness ratio is manually calculated and the value of P_b is computed empirically through graphs and plots.

At lower Mach number C_D the exhibits a higher value although it decreases as the fineness ratio is increased. However, the rate of decrease of the drag reaches its maximum at fineness ratio 3 after that the change in C_D is not so apparent. Also increasing the Mach number also results in a noticeable decrease in the drag. Figure-21 displays the behavior of the skin friction drag that increases in proportion with the fineness ratio. This is consistent with

Second equation that contains the variable S_w which is the wetted area. By increasing the fineness ratio, the geometry of the nose also increases and thus leads to an increase in surface area. It can be noted that the base drag is independent of the shape and fineness ratio of the nose. It is only affected by the base diameter and Mach number which also in turn influences the base pressure.

On referring to Fig-20, we can state that wave Drag, C_{WV} as a function of fineness Ratio and Mach number.

The plot demonstrates that the change in wave drag is mostly affected by the fineness ratio. As the fineness ratio increases the wave drag decreases. This agrees with the logic that an increased fineness ratio makes the nose more slender where it is able to stay in the Mach cone with minimal air disturbance. When compared to the skin friction drag, the drag coefficient values in general are much higher especially at low fineness ratios.

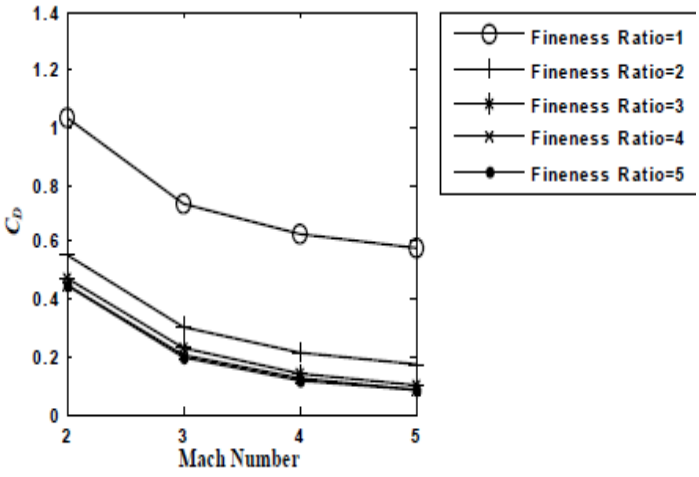

Fig-18 Variation of C_D with Mach & Fineness ratio

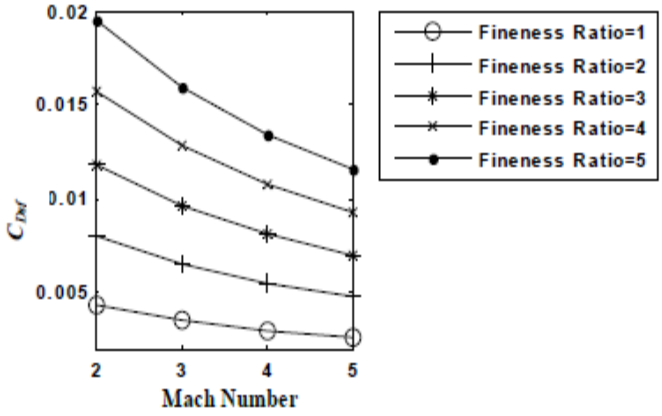

Fig-19 Variation of skin friction with Mach & fineness ratio

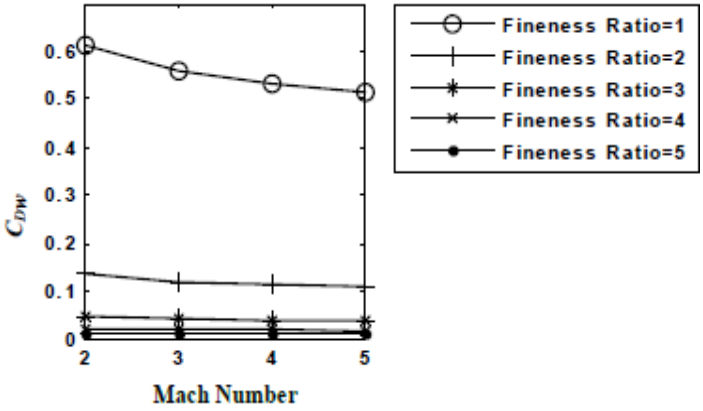

Fig-20 Variation of wave drag with Mach & fineness ratio.

From the above plots we can clearly see that skin friction component of drag increases as fineness ratio is increased, but if we view from totality the total value of drag does not change significantly, if the fineness ratio is increased significantly then the total drag may increase as skin friction component of the drag increases manifolds. At low Mach & fineness ratio wave drag contributes significantly, base drag is a function of Mach number but is less significant for supersonic analysis. Wave drag is a major contributor and as designer we must bring it to an optimal value, but must be careful with changes associated with the fineness ratio.

5. NOSE CONE FOR HYPERSONIC REGIME

The study of hypersonic flows is generally done for blunter nose cone profiles, the application of sharper nose cone profiles is restricted for this flow regime, due to its adverse heat transfer characteristics. Due to the use of blunted profiles for the regime we need to look into the shock characteristics, shock wave shape and detachment distance. Aerodynamic characteristics and heating also have to be extensively looked into.

For the purpose of looking into the relation of geometric properties and the aerodynamic characteristics associated we refer to some experimental and numerical results mentioned below:

1. For a spherically blunted nose cone there is existence of minimum pressure instantaneously downstream of the nose-cone junction for a semi-cone angle of 40°, whereas it is positioned far downstream for a smaller semi-cone angle of 20°. It was observed that the shock detachment distance between the bow shock and the blunted nose cone surface varies linearly with the nose radius.
2. Multi- step base missile bodies for flow of Mach 5.78 showed an 8% reduction in overall drag.
3. On investigation of bluntness ratio and their effect on the aerodynamic characteristics it can be found

that its effect on blunt nose cones with large semi cone angles is negligible as compared to smaller ones.

4. It was observed that for higher Mach numbers the effect of bluntness ratio was significant for normal force coefficient, fore body drag coefficient for smaller semi- cone angles. For angles less than 30° centre of pressure location is more sensitive than Mach number. For angles above 35° the location is affected more by Mach number changes than bluntness ratio.
5. For a Mach number range of 1.24 to 7.4 at a pre-determined Reynolds number, the diameter of the spherical tip does not increase fore-body drag.
6. For blunted bodies in hypersonic flows, there is a presence of low total pressure layer near the blunted surface surrounded by a high total pressure layer, this was due to the inflection of shock, indicating 3-D flow characteristics.
7. Heat transfer characteristics can be enhanced by the use of fins for a particular stagnation enthalpy and Mach number.

The modification in the flow and shock structures, plays a vital role in enhancing the drag and heat flux reductions, it finds numerous applications in the design of high speed aerodynamic vehicles. The shock detachment distance decreases with an increase in fitness ratio, as if we logically see that with an increase in fitness ratio the body tends to be more slender, hence reducing the detachment distance.

In the subsequent discussion we would be looking into the numerical simulation of spherically blunted and parabolic nose cones with fitness ratios of 4.7 and 3.6

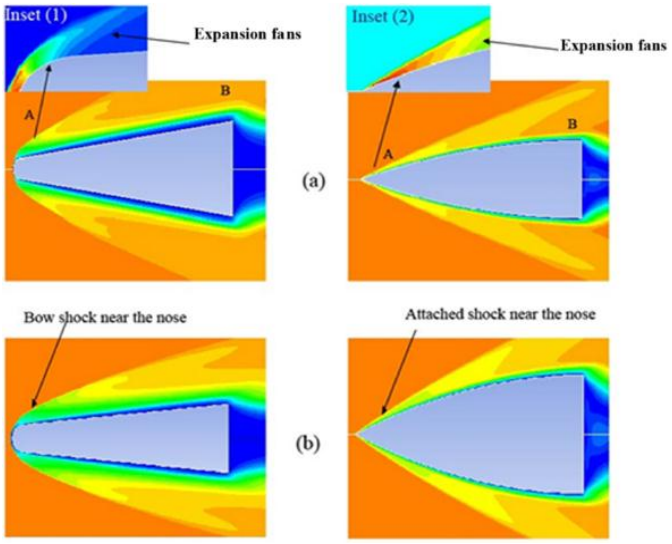

Fig-21 Shock structure and detachment for (a) 4.7, (b) 3.6 fitness ratios, on the left is spherically blunted nose cone and on the right is parabolic.

The bow shock wave is normal to the flow direction near the nose and the flow passes through it without turning and comes to rest when it reaches the nose. The shock wave is inclined to the flow direction, it is oblique above and below the normal shock which helps the flow turn so that it can flow parallel to the nose cone surface. The flow turning is further assisted by the presence of **expansion waves** which is formed at the vicinity of the nose tip. This can be noticed for the attached shock in the parabolic nose profile also, but the slight difference in this case is that the expansion fans are formed at the **curved surface** following the oblique shock. As the flow reaches the cone base the flow has to be turned parallel to the axis so this is achieved through **expansion fans** which is formed at the cone base for both cases. The flow acceleration and deceleration can be understood through the vector fields. In the case of **spherically blunted** nose cone the flow decelerates due to the **strong normal shock**, but then accelerates sideways along the profile through oblique shocks and a series of expansion waves. The similar mechanism is followed for the **parabolic profile** the only subtle difference is that the deceleration does not happen due to normal shock formation. In both spherically blunt and parabolic profiles a strong **recirculation zone** is observed behind the base.

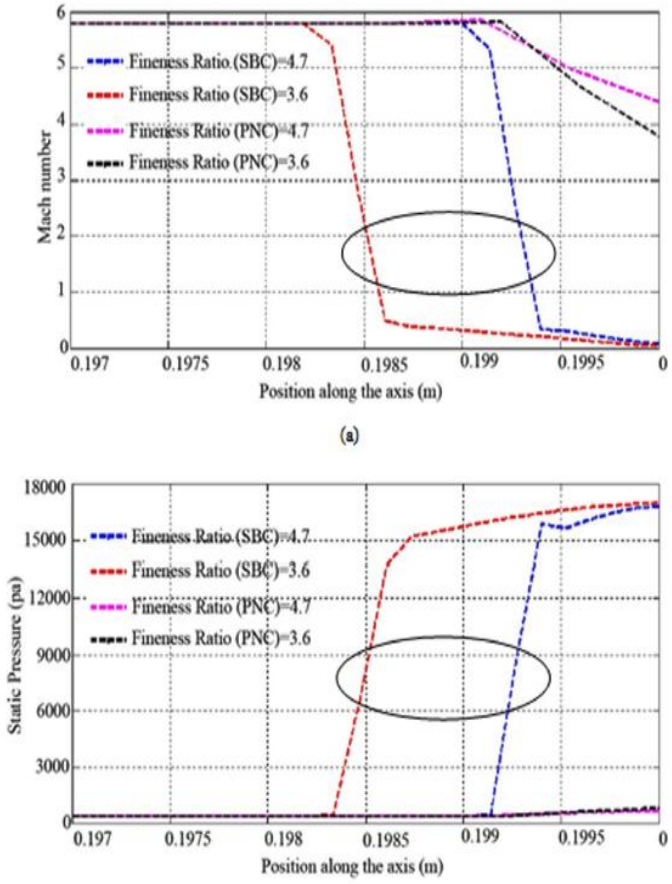

Fig-22 Plots of static pressure and Mach number variance with axis, elliptical region showing sharp rise in both quantities.

The location of the bow shock near the spherically blunted nose cone is represented by a sudden jump in the Mach number and static pressure plots, a smaller jump is observed for a parabolic nose cone. This jump in quantities can be explained due to the presence of detachment distance for spherically blunt bodies causing a sharp change in slopes of Mach number and static pressure plots, in the case of a parabolic profile there is no detachment distance present. The presence of very low static pressure in the parabolic nose cone, may be the reason for reduction of low drag as compared to the spherically blunted cone.

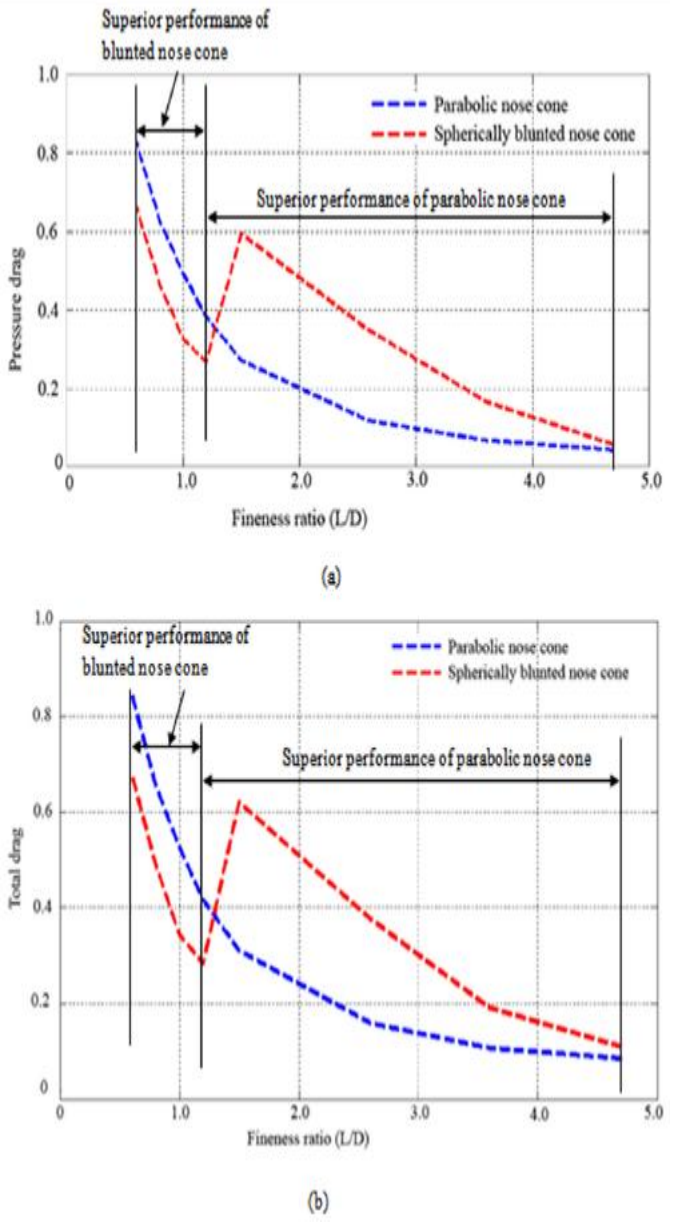

Fig-23 Plots showing the performance comparison for both spherically blunt & parabolic nose profiles for various fitness ratios.

From observing the above plot it can inferred that for a Mach number range of 1-5 **parabolic nose** shape is preferred, than **spherically blunt profiles**. But since we are talking about hypersonic flows we need to consider the effect of heat transfer and must resort to blunter bodies.

The variation of **heat flux** for both the nose profiles is somewhat similar, the heat flux is **higher** near the **stagnation point** and gradually **decreases** along the wall as we traverse axially and then remains **constant**. The heat flux for **parabolic nose** cones is much lesser than that of **spherically blunt** ones due to **shock structure** or maybe the **boundary layer interaction**.

If reducing the drag alone is of prime importance, then the **sharp cone configuration** could be chosen even though they provide **lesser heat flux reductions** when compared to other configurations. In case of **blunt bodies**, even though heat flux generated is less, higher drag is experienced. For all values of nose radius, with increase in Mach number the C_D value decreases. With increase in **angle of attack**, the C_D value increases for all Mach numbers. This study can be extended in multiple directions by considering other configurations, different free stream conditions and other design and analysis parameters.

6. CONCLUSIONS

The following plot is the best quantitative method to compare the performance of various nose cone designs for different flow regimes.

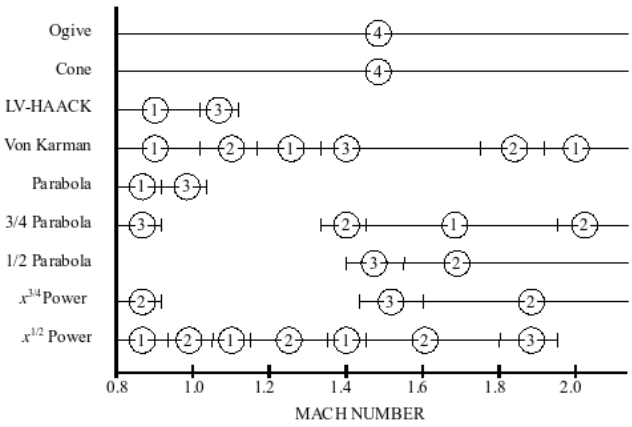

Fig-24 A quantitative comparison of drag characteristics 1. Superior, 2. Good, 3.fair, 4. Inferior, for different nose cone profiles.

As discussed above **elliptic nose cone** shape is preferable for a **subsonic flow regime**, where **Von Karman** is preferred for slightly above **subsonic to transonic**. For **supersonic flow** more than the design it is a compromise between the different kind of drags, whereas in **hypersonic flow** the **aerodynamic heating** is a crucial problem and the

geometric parameters of the nose cone have to selected in accordance.

REFERENCES

[1] Drag of Conical Nose at Supersonic Speeds Arthur S.Q Saw*, Abdulkareem Sh. Mahdi Al-[2]

[2] Obaidi Department of Mechanical Engineering, School of Engineering, Taylor's University, Malaysia.

[3] Hypersonic flow past nose cones of different geometries: a comparative study

Ashish Narayan, S Narayanan and Rakesh Kumar.

[4] Influence of Nose Radius of Blunt Cones on Drag in Supersonic and Hypersonic Flows A. Hemateja et al 2017 IOP Conf. Ser.: Mater. Sci. Eng. **225** 012045

[5] Nose cone and design of avion A.Yeshwanth, PV.Senthiil.